NASA TM X- 70520

AEROSOL SCATTERING OF ULTRAVIOLET SUNLIGHT IN THE TROPICAL MARITIME ATMOSPHERE

A. GHAZI
A. J. KRUEGER
R.S. FRASER

NOVEMBER 1973

GSFC —— GODDARD SPACE FLIGHT CENTER ——
GREENBELT, MARYLAND

AEROSOL SCATTERING OF ULTRAVIOLET SUNLIGHT

IN THE TROPICAL MARITIME ATMOSPHERE

A. Ghazi

A. J. Krueger

R. S. Fraser

November 1973

GODDARD SPACE FLIGHT CENTER

Greenbelt, Maryland

AEROSOL SCATTERING OF ULTRAVIOLET SUNLIGHT

IN THE TROPICAL MARITIME ATMOSPHERE

A. Ghazi, A. J. Krueger and R. S. Fraser
NASA/GSFC, Greenbelt, Maryland

ABSTRACT

The effects of atmospheric aerosol scattering on the vertical profile of solar ultraviolet radiation at $\lambda \simeq 3200\text{Å}$ are investigated. Measurements of diffuse and total (diffuse and direct) ultraviolet radiation were made using a rocket-borne optical sonde in the marine atmosphere of Antigua ($17.2°\text{N}$, $61.8°\text{W}$). During observations, the sun was at zenith. Vertical profiles of directly transmitted solar radiation are calculated by subtraction of the diffuse component from the total radiance. Using these values of direct downward solar uv-flux, the optical thickness of the atmosphere is derived as a function of altitude. Absorption by ozone is also considered. In the troposphere the values of observed optical thickness are in general equal to or lower than those expected theoretically from Rayleigh scattering alone. These low values of ultraviolet extinction can be explained in terms of strong forward scattering by Mie-type atmospheric particles. The measured radiation profiles are compared with those computed for a multiple scattering model atmosphere. Some computations regarding the interaction of uv-sunlight with maritime aerosols are presented.

CONTENTS

Page

AEROSOL SCATTERING OF ULTRAVIOLET SUNLIGHT

IN THE TROPICAL MARITIME ATMOSPHERE

1. INTRODUCTION

Atmospheric ozone has been studied systematically during the last five decades but the observational data on the vertical attenuation of ultraviolet sunlight by atmospheric aerosols are rather limited. The aerosol scattering optical thickness of the atmosphere in ultraviolet has been reported to either increase (Guschin 1968), or decrease (Rodionov et al. 1942) with wavelength, or even become negative (Pettit 1932). This problem is of significant interest not only for the accuracy of ozone measurements but also for obtaining valuable information about the optical properties of aerosols in the ultraviolet. Recently, Roosen et al. (1973) have investigated worldwide variations in the atmospheric transmission through analysis of solar radiation measurements taken during the first half of the twentieth century at thirteen widely separated stations. Their reported extinction in the ultraviolet for many sites was found to be equal to or lower than that expected from Rayleigh scattering alone. Deirmendjian and Sekera (1956) had suggested that the observed low extinction values of solar ultraviolet radiation, usually found at coastal stations, were partly due to the presence of Mie-type particles with extremely high forward scattering characteristics. Ground-based measurements of ultraviolet sky radiation made at Cologne (W. Germany) with a narrow-angle scanning photometer (Ghazi 1973)

also indicated negative values of aerosol optical thickness in the region 3100-3600Å. Since the solar radiation in this region is absorbed by atmospheric ozone and is to some extent biologically active, it is interesting and useful to study the effect of aerosols on the uv-sunlight.

In the present paper an attempt is made to investigate the effect of non-absorbing atmospheric aerosols on the downward solar radiation at $\lambda \simeq 3200\text{Å}$ at selected levels of the tropical maritime atmosphere. Measurements of ultraviolet solar radiation were made at Antigua (17.2°N, 61.8°W) using a rocket-borne optical sonde (Krueger and McBride 1968). During the descent of the sonde in the atmosphere, the sun being at zenith was obscured by its parachute from time to time. Thus during obscuration only the scattered ultraviolet sky-light was measured by the rocket-borne and parachute suspended optical sonde. Vertical profiles of direct solar radiation at 3205Å and 3220Å are obtained by subtracting the scattered component from the measured (direct + scattered) total radiance. These direct uv-flux profiles are then used to calculate the total scattering optical thickness of the atmosphere up to an altitude of 20 km. The measured uv-radiation profiles are compared to the theoretically predicted vertical profiles of rocket-sonde measurements. In order to further investigate the optical characteristics of atmospheric aerosols interacting with uv-sunlight, computations are performed for "realistic model atmosphere" and some significant results are presented.

2

2. METHOD OF MEASUREMENT AND DATA REDUCTION

The experimental technique of the rocket sonde, which is primarily employed for the measurement of vertical profile of atmospheric ozone, is very similar to one developed by Paetzold (1961) and has been described elsewhere (Krueger 1969). It would suffice to state here that the optical sonde is equipped with four narrow-band filters with their transmission centered at wavelengths between 2650-3250Å. For the determination of ozone profiles wavelengths smaller than 3000Å are mainly used. The light collector is a small integrating sphere provided with a wide field of view to avoid the problems of pointing with varying solar zenith angles (Fig. 1a). The variation of angular response of the light detector is illustrated in Figure 1b. The radiation is received at uniform response between $0° < \theta < 60°$ and the response gradually decreases towards the horizon.

Measurements of ultraviolet radiation are made, as mentioned earlier, during the descent portion of the flight when the rocket-borne optical sonde is suspended by a parachute from an altitude of about 50 km downward to the surface. The signal received on the ground at about every one second for the $\lambda \simeq 3200Å$ filter is converted to digital form for computer analysis.

Measurements of two rocket flights made at Antigua on May 16, 1972 (Flt. 1) and May 23, 1972 (Flt. 2) are discussed here. The peak altitudes reached were around 50 km. The meteorological conditions at the time of the flights were for
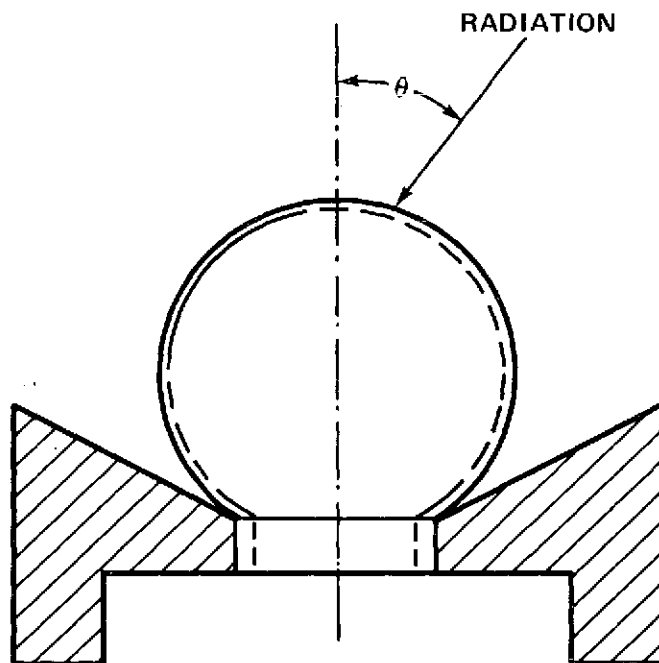
3

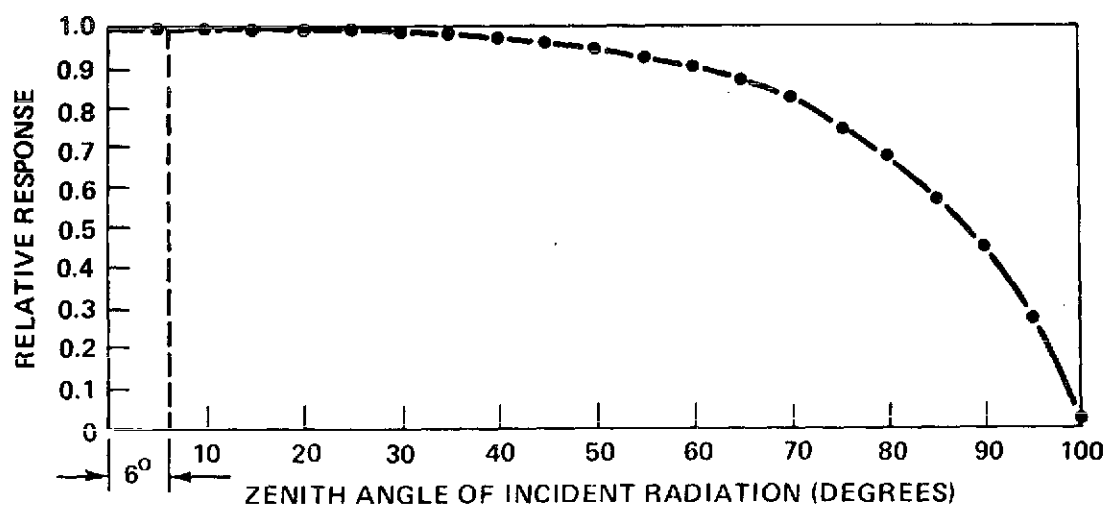Figure 1a. Schematic view of the light collector

Figure 1b. Angular response function of the rocket-sonde's light collector

4

Flt. 1: Scattered Cu clouds (1/8) at 23-2400 ft. Winds 5 kts from east, Visibility 30 km. Relative humidity 75%.

Flt. 2: Scattered Cu + Sc clouds (2/8) at 2300 ft. Winds 6 kts from southeast, Visibility ~30 km. Relative humidity 76%..

The position of the sun during the period of the descent of the sonde in the lower stratosphere and troposphere on both days of flights remained around zenith (solar zenith angle $Z \sim 0° - 6°$). Obscuration of the solar disk by the parachute subtending a half angle of $6°$ was therefore possible during most of the portion of descent through the troposphere and lower stratosphere. In the present study only the measurements made with the $\lambda \simeq 3200\text{Å}$ filter will be discussed since the diffuse radiance measurements at wavelengths $\lambda < 3200\text{Å}$ are strongly affected by multiple scattering and ozone absorption so that the signal to noise ratio becomes critical.

The total radiation F_T received by the light collector is given by F_T (μw cm^{-2} Å^{-1})

$$F_T = 2\pi \int I(\theta) R(\theta) \sin\theta \, d\theta \tag{1}$$

where

$F_T = F_D + F_s$ and $F_s = F_s' + F_s^*$

$F_D =$ Flux of directly transmitted radiation

$F_s =$ total scattered radiation received from the sky hemisphere

$F_s' =$ scattered radiation measured with the obscured sun
(i.e. $\int_{\theta=0}^{6°} R(\theta) \sin\theta \, d\theta = 0$)

$F_s^* =$ scattered radiation for $\theta \leqslant 6°$ of the solar disk (aureole contribution)

$I(\theta)$ = intensity of incident radiation

$R(\theta)$ = response function of the light collector

The individual measured values of F_s' are at maximum about 50% of the total (F_T) radiation measured at the same altitude. In this way it is easy to separate the scattered component of the measured radiance from the total. Radiation vs height curves are obtained for both of the measured values. Although the data are computer generated the final smoothing is done by a manual fit which we believe is least subject to error. Radiation vs height curves include some erroneous points. Possible error results mainly due to the instability of the parachute, inhomogeneity in the wall of the integrating sphere and the change in sensitivity of the photomultiplier caused by the temperature variations in the atmosphere. By fitting a curve manually to the computer generated data points, the error due to parachute instability and inhomogeneity of the light detector is reduced to a large extent. The measured curves are corrected for about 3% response variation of the photomultiplier. Consequently, we estimate the effective error in the measurements to be $\leq 4\%$. The effective transmissions of the filter used in the two flights were calculated. The peak transmission of the filter used in Flight 1 was centered at $\lambda = 3220\text{Å}$ with a half-width of 50Å. The filter transmission for Flight 2 peaked at $\lambda = 3205\text{Å}$ with 45Å half-width.

3. RESULTS

The values of measured radiation at 3220Å and 3205Å as a function of altitude are depicted in Figures 2 and 3. Curves labeled 1, 2 and 3 represent scattered (F'_s), direct (F_D) and total (F_T) radiation profiles. The downward direct solar flux profile (F_D) is obtained firstly by subtracting the values of scattered radiation (F'_s) from the total (F_T) at every 1 km interval beginning from 45 km downward to the surface. Secondly, since this difference includes the contribution due to aureole (F^*_s) (see eq. 1) the values were corrected to derive the direct flux profile. Figure 4 allows determination of the computed contribution by aureole (F^*_s) to the scattered radiation of the sky as a function of altitude (see section 4 and 5). Aureole contribution at the surface is about 2.8%. The direct solar ultraviolet flux profiles are thus obtained according to equation:

$$F_D = F_T - (F^*_s + F'_s) \qquad (2)$$

and shown in Figures 2 and 3 as Curve 2. Bars indicate the range of error in observation. Figures 2 and 3 show that the measured scattered radiation increases with increasing optical depth of the atmosphere. The change in slopes of Curves 1 from about 20 km downwards is evident. This may be attributed to the Rayleigh scattering becoming appreciable at that level whereas the ozone absorption decreases rapidly from 20 km to the surface. Nevertheless the response characteristics of the light detector are also to some extent responsible for this behaviour of scattered radiation profile. As the sonde descends
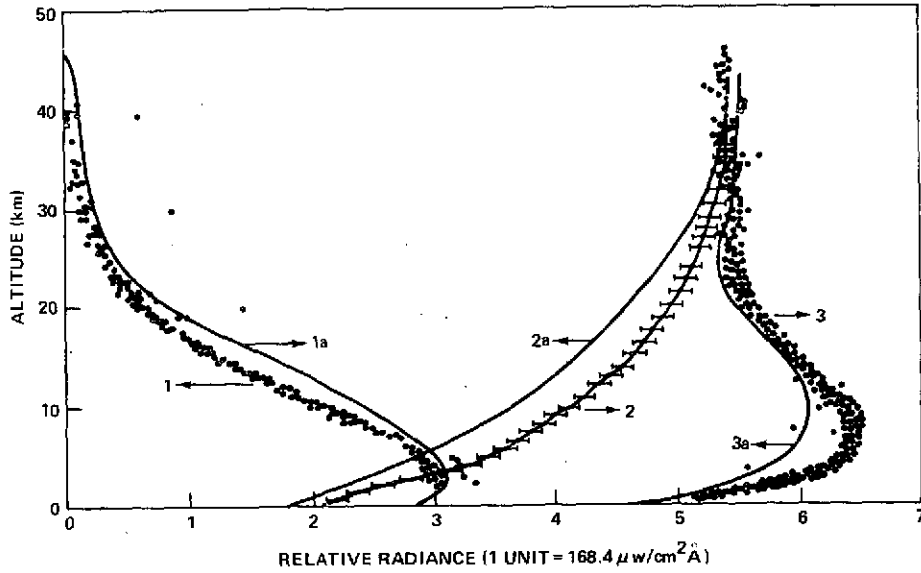
7

Figure 2. Observed and computed vertical profiles of uv-radiance at 3220Å. Curves 1, 2 and 3 are measured scattered, direct and total radiation profiles respectively. Corresponding computed profiles are labeled 1a, 2a and 3a. Solar zenith angle $Z = 0°$, albedo $a = 0.06$. Computation parameters are defined in Fig. 6a, 6b, 9, 10a
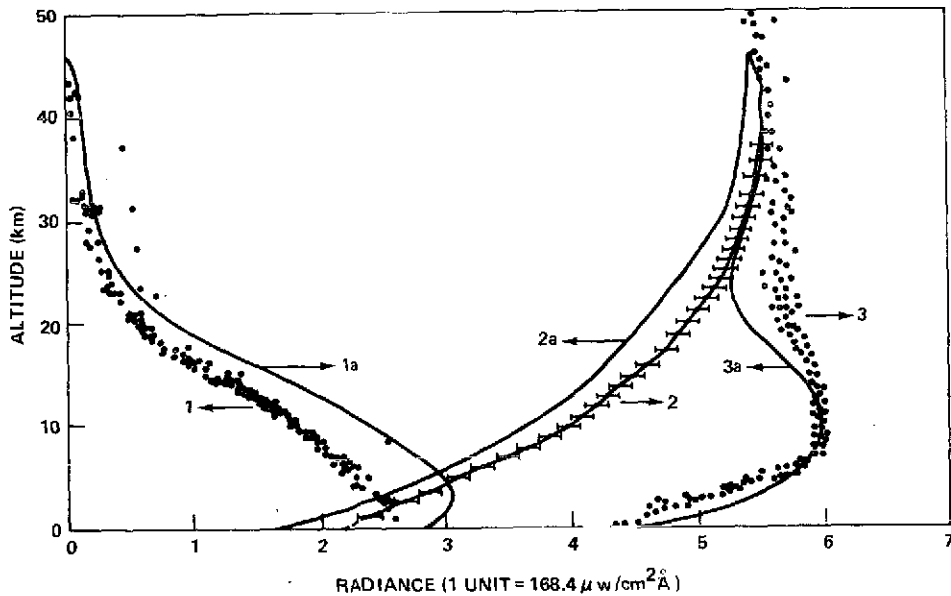

Figure 3. Observed and computed vertical profiles of uv-radiance at 3205Å. Definitions and parameters are same as in Fig. 2

8

into the multiple scattering layers of the atmosphere, the light detector receives more light from the angles $\theta \geqslant 90°$, thereby enhancing the total radiation (Curve 3). A maximum in Curve 3 is reached near a level in the troposphere from where the direct component begins to decrease rapidly due to strong scattering and quickly increasing optical depth. It is interesting to see that the mentioned maximum in Curve 3 (Fig. 2) has a value about 17% higher than that observed at the top of the atmosphere ($\sim$ 45 km). Only at about an altitude of 2 km the measured total radiation reaches a value equal to that measured at 45 km height. The strong decrease of measured total radiation in the middle and lower troposphere is certainly due to molecular and aerosol scattering since the ozone absorption in these layers of the atmosphere becomes insignificant. An interesting feature of the scattered radiation profile (Curves 1) is the sudden change of slope at about 3 km altitude. The measured scattered
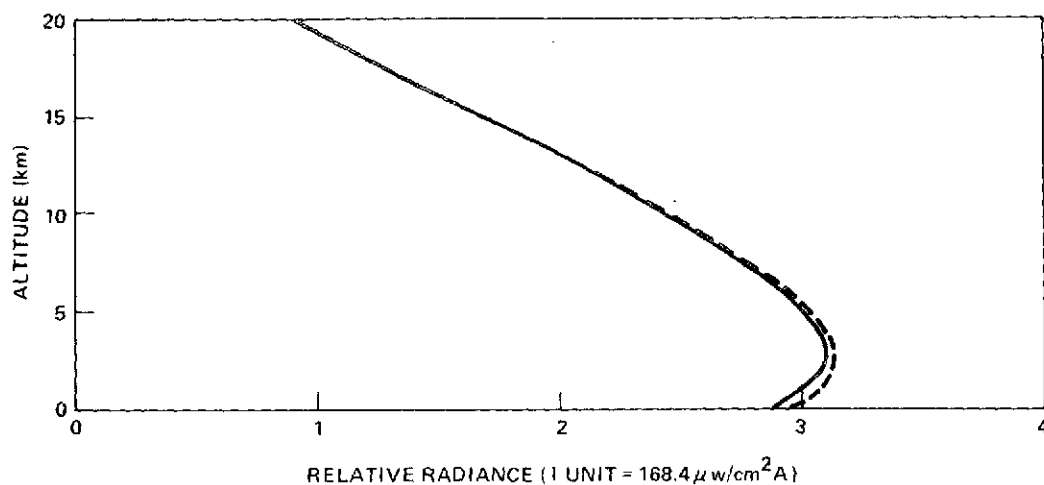

RELATIVE RADIANCE (I UNIT = 168.4μ w/cm^{2}A)

Figure 4. Computed profiles of uv–radiance at λ = 3200Å expected to be measured by the rocket-sonde with (solid line) and without (dashed line) obscuration of the sun ($\theta \leqslant 6°$). Parameters are same as in Fig. 2 caption

radiation seems to change very little from about 2.7 km downward to the surface. The reason for such a behaviour is due to the total optical thickness of the atmosphere reaching a value $\geqslant 1$, after which no increase in diffuse radiation is to be expected as supported by the model computations. Moreover, the atmosphere near the oceanic surface would not enhance the scattered component very much since Georgii and Gravenhorst (1972) report that the concentration of background aerosol near the surface of the Atlantic Ocean is almost equal to the aerosol amount found in the middle troposphere of the continents ($\sim$300 particles/cm^3). Furthermore, the contribution of reflected uv-radiation from the ocean's surface is expected also to be very small ($\sim 6\%$) according to measurements made by Furukawa and Heath (1973).

Figures 2 and 3 show that the derived direct flux profiles are almost equal in their values at λ = 3205 and 3220Å. The measured direct flux at these wavelengths is seen to be depleted by about 66-67% from the level at 45 km (1.6 mb) to the surface. The attenuation of direct radiation in the biosphere (3.06 km downwards) is very similar in magnitude to that computed by Braslau and Dave (1973) for a realistic model 'C' of their study. Extinction of direct uv-sunlight due to air molecules and aerosols is measured to be very strong in the troposphere and is much higher in magnitude than caused by ozone absorption alone in the stratosphere.

Figure 5 allows the comparison between computed vertical profiles of the Rayleigh optical thickness $\tau_R = \int\limits_{h=0}^{45\,km} \tau(h)\,dh$ at 3205Å and 3220Å and the scattering
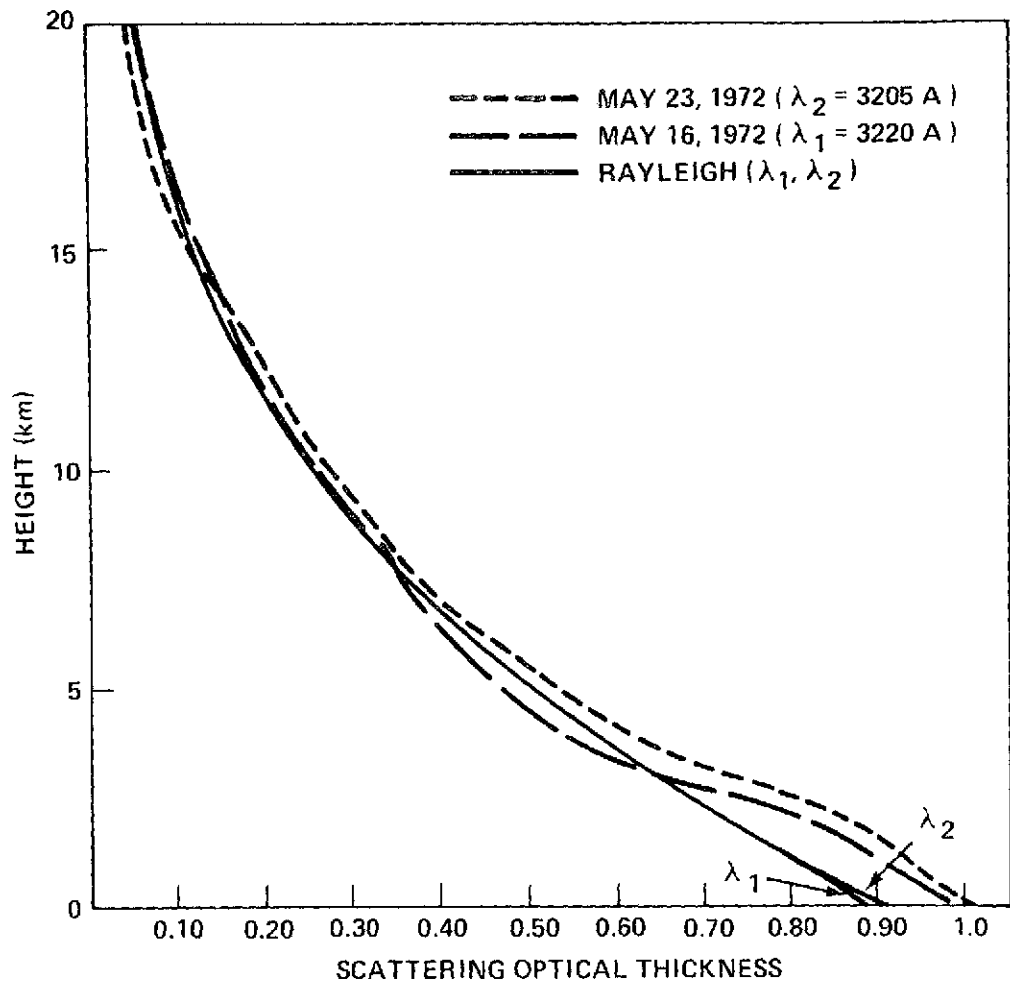
10

Figure 5. Comparison of measured values of scattering optical thickness τ_s and computed Rayleigh optical thickness τ_R at 3205Å and 3220Å

optical thickness τ_s of the atmosphere calculated from the derived values of direct solar flux profiles.

$$\tau_s = \tau - \tau_{O_3} \quad \text{where}$$

$$\tau = \tau_R + \tau_A + \tau_{O_3}$$

(3)

τ_R = Rayleigh optical thickness

τ_A = aerosol induced scattering optical thickness

τ_{O_3} = ozone absorption optical thickness $\alpha \cdot u(h)$

α = abs. coefficient of ozone cm^{-1}

$u(h)$ = total amount of ozone at altitude h (atm-cm)

The values of Rayleigh scattering optical thickness were calculated from the theory and corrected for the filter transmission. The effective values of τ_R at 3205Å and 3220Å are 0.906 and 0.887 respectively. For the calculation of ozone absorption optical thickness, the rocket-measured values of ozone distribution from 50 to 15 km altitude and the values given by McClatchey et al. (1971) for standard tropical atmosphere from 15 km to the surface were used (Figure 6a). For both days of flight the total amount of ozone in the atmosphere was calculated to be 0.277 ± 0.002 atm-cm O_3.
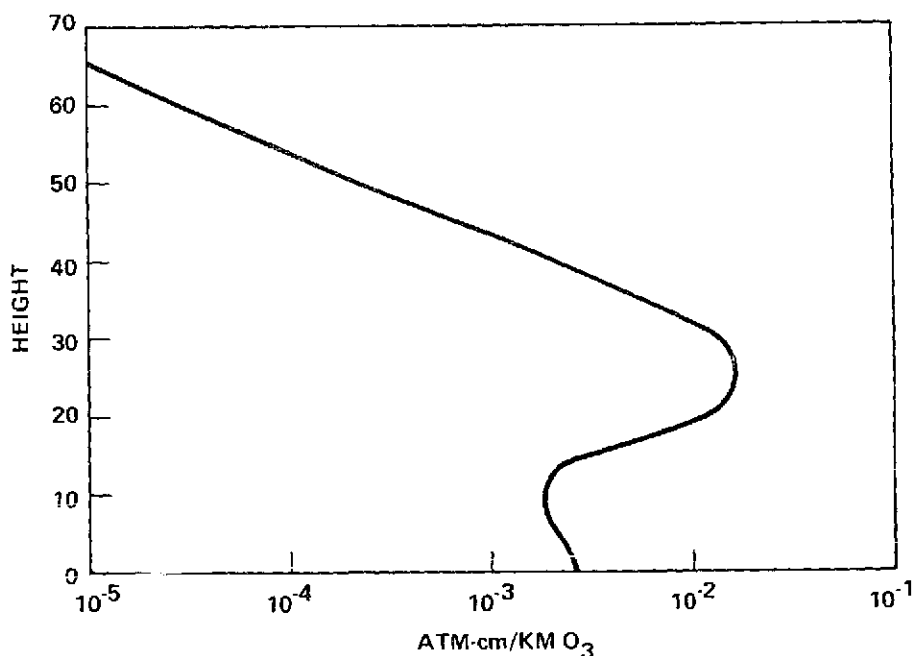

Figure 6a. Vertical profile of atmospheric ozone used for computing radiance profiles. Total ozone = 0.277 atm-cm

12

For the derivation of aerosol optical thickness $\tau_A(h)$ as a function of altitude we used a simple relation:

$$\tau_A(h) = \frac{1}{M}\left\{(\ln F_O - \ln F_D(h)) - \alpha \cdot u(h) - \tau_R(P/P_O)\right\} \qquad (4)$$

F_O = flux at the top of the atmosphere (1.6 mb)

$F_D(h)$ = measured value of direct solar radiation at height h

α = effective absorption coefficient of ozone at λ = 3205 and 3220Å;

$\alpha(3205\,\text{Å}) = 0.640 \text{ cm}^{-1}$; $\alpha(3220\,\text{Å}) = 0.568 \text{ cm}^{-1}$

$u(h)$ = total amount of ozone at altitude h

M = air mass (in our case $M=1$, while $Z=0°$)

P/P_O = ratio of measured pressure at a level to the pressure at the surface.

The values of aerosol induced scattering optical thickness at the surface for the days of Flights 1 and 2 are calculated to be respectively 0.10 and 0.14, which are relatively low.

As it can be seen from Figure 5, the values of total scattering optical thickness are generally lower or equal to the Rayleigh scattering optical thickness. In other words aerosols either contribute very little to the extinction of ultraviolet sunlight or they may even enhance the measured value of radiation to an extent higher than that expected from the molecular scattering and ozone absorption theory. We believe that these low values of uv-extinction are due to strong forward scattering by large particles present in the maritime atmosphere of Antigua. Further support to this conclusion is furnished by comparing the measured profiles of radiation with those computed using a realistic theoretical model of the atmosphere.

4. COMPARISON OF MEASUREMENTS WITH THEORY

The measured profiles of ultraviolet radiation can be compared to the computed radiance profiles shown in Figures 2 and 3. The curves 1a, 2a, 3a are computed using the computer programs for the calculation of radiation flux developed by Dave (1972). The computations are made for a cloudless, plane-parallel semi-infinite atmosphere taking into account all orders of scattering. Vertical concentrations of ozone and aerosol are specified and are represented in Figures 6a and 6b. Details of computation are given in section 5.

In order to compare our measurements with the theory we modified the flux calculations according to eq. 1; thus taking the response function of the used light detector into account. This consideration is important because the measured radiation profiles are different than the "flux" profiles (radiation
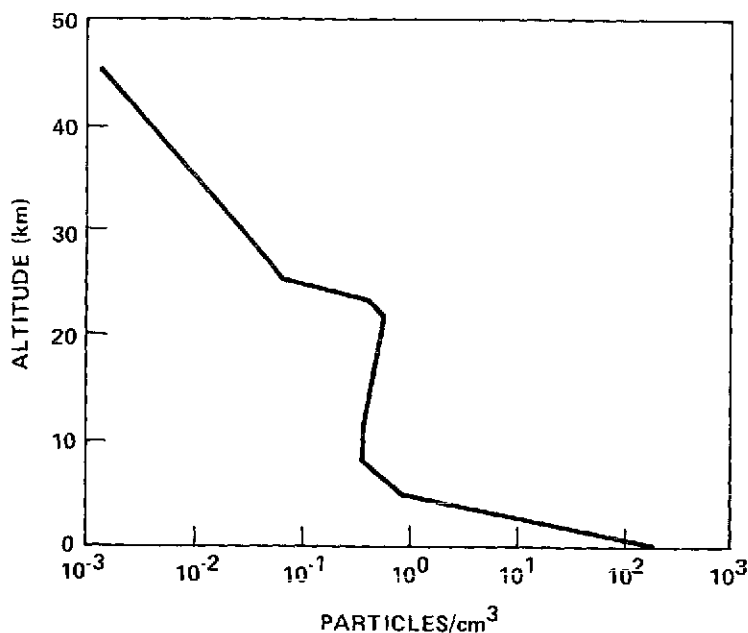

Figure 6b. Aerosol height distribution adopted for calculations. Total number of particles in one cm^2 column is 1.4×10^7

incident on a horizontal surface $F = 2\pi \int I(\theta) \cos\theta \sin\theta \, d\theta$) which can be theoretically expected at the used wavelengths. Figure 7 illustrates the difference between computed profiles at $\lambda = 3200\text{Å}$ using the response function of the light detector and the computed flux profiles. As can be seen from Figure 6, the shape of the curves (1, 1a and 3, 3a) of the scattered and total radiation incident on a flat plate and an integrating sphere are dissimilar. The flux profile (3) does not show a maximum in the troposphere which is a characteristic of the radiation profile measured by the rocket-payload. Both scattered and total radiation profiles (curve 1a and 3a) show a higher value than the computed flux profiles. However it is interesting to note that the downward direct solar uv-flux remains the same in both cases.
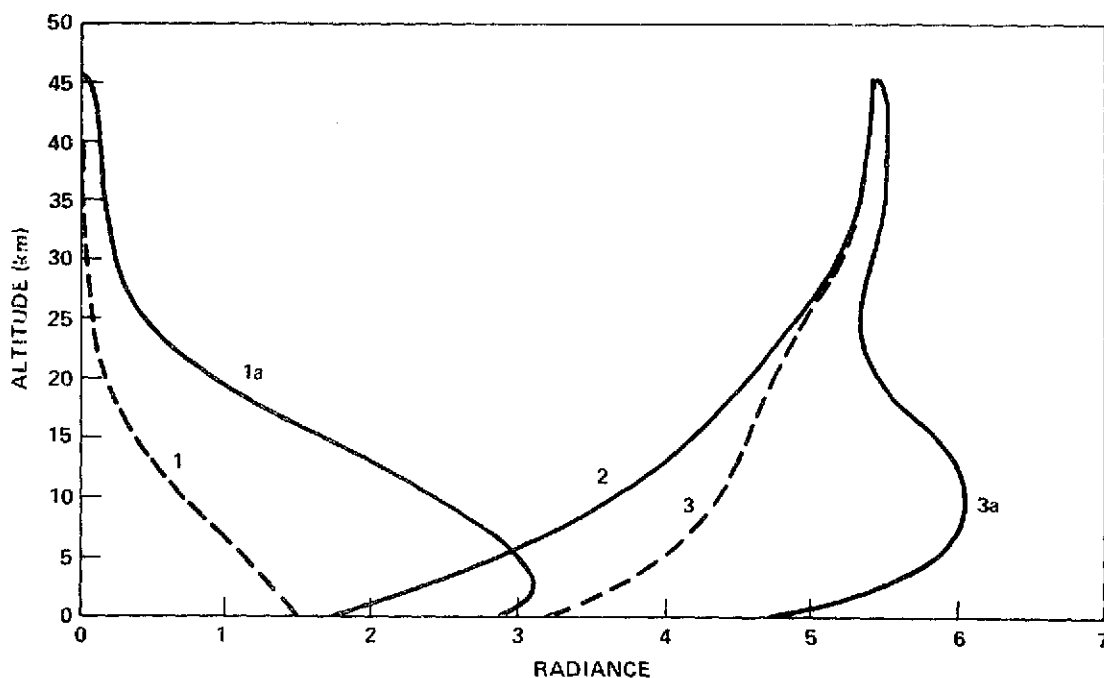

Figure 7. Comparison between computed profiles of radiances and theoretical 'flux' profiles. Curves 1a, 3a are computed scattered and total radiances as expected to be measured by rocket-sonde. Curves 1 and 3 are corresponding scattered and total 'flux' profiles at 3220Å. Curve 2 is computed direct flux profile

The excellent agreement between the theoretically expected and measured vertical profiles of radiances is evident from Figures 2 and 3. The maxima of total radiance profiles appear at almost the same level (~ 10 km). One can also see a conformity between the observed and computed levels where the values of direct flux and diffuse component become equal (~ 5-6 km). The computed scattered radiation curve shows a stronger bend from about 3 km downward to the surface than the measured profile of scattered radiation. The direct solar flux profiles, derived from the measurements, show somewhat higher values of radiance than the computed profiles. Especially in the upper troposphere the bias between the two curves (2 and 2a) is appreciable. This cannot be entirely due to difference in ozone absorption optical thickness observed and computed at those levels, since even if ozone absorption is neglected the computed flux profiles show a lower value and the discrepancy remains. The reason for this dissimilarity is not well understood. It seems that we are dealing here with aerosol layers of different spectral properties in the ultraviolet. Experimental evidence regarding the existence of some peculiar aerosol layer in the troposphere with 'anomalous' behaviour of spectral attenuation coefficient in ultraviolet was given by Rodionov (1950). The higher radiance values of derived solar flux profile lead to the calculation of low extinction values of ultraviolet sunlight and relatively low value of aerosol induced optical thickness (Fig. 5). There seems to be theoretical evidence that forward scattering by large particles would increase the direct solar flux as

compared to the diffuse component. In order to study the characteristics of

polydisperse non-absorbing and purely scattering atmospheric aerosols inter-

acting with ultraviolet sunlight at $\lambda = 3200\text{Å}$, we have performed computations

some of which are presented and discussed in the next section.

5. COMPUTATIONAL DETAILS

Models of the atmosphere used for the computations given here are for

cloudless sky and include 0.277 atm-cm of total ozone and an aerosol height

distribution similar to "Average dust" model as given by Braslau and Dave

(1973). Particle number density varies with a strong exponential decrease

from the surface to about 5 km and then remains fairly constant to about 17 km

and a layer of higher concentration (Junge Layer) is centered at around 23 km

altitude. Number of particles in a cm^2 column is taken to be 1.4×10^7 corre-

sponding to an aerosol optical thickness of 0.13 which is comparable to the

derived values from the radiation measurements.

The size distribution functions used for our computations are represented

in Figures 8 and 9. Figure 9 is obtained by fitting a log-normal distribution

to the maritime aerosol size distribution function as reported by Eiden and

Eschelbach (1973) and has been normalized to one particle/cm^3 for representa-

tion. The mode radius is 0.2μm. Figure 8 is representative of mid-latitude

continental aerosol size distribution. This discontinuous distribution has a

maximum constant range of particles with radius $r = 0.03 - 0.1 \mu$m after which
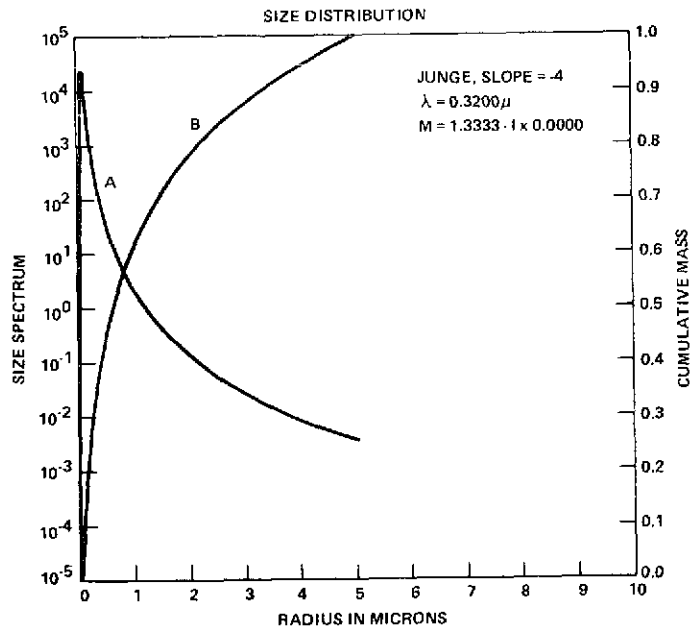
Figure 8. Aerosol size distribution (continental): Curve A. Curve B represents cumulative mass of aerosols as a function of radius. Ordinate at left is dn/dr
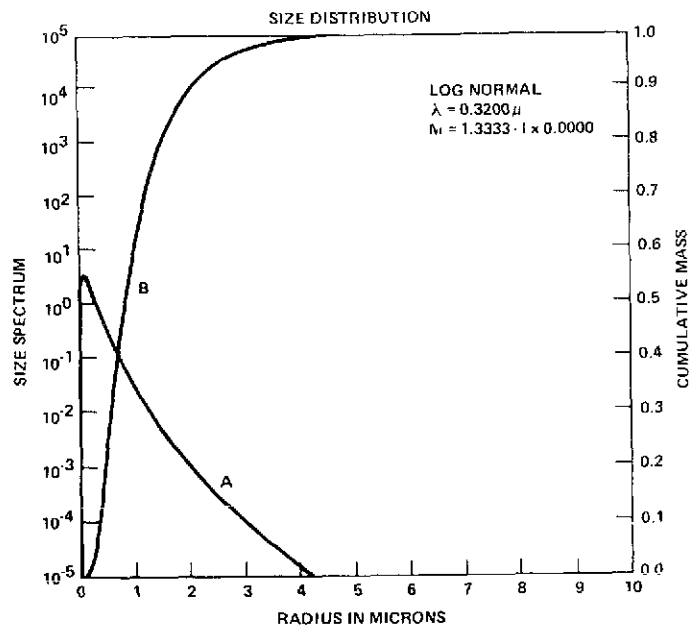

Figure 9. Maritime aerosol size distribution used for the computation of radiance profiles is normalized to 1 particle/cm³. Ordinate on the left is dn/dr. n = number of particles cm⁻³, r = radius of particles. Curve B is as defined in Fig. 8

the distribution is based on power law with Junge exponent $\nu^* = 3$ and an arbitrary cut-off at $5\,\mu m$. Assuming the low altitude particles to be mainly water-coated in the marine atmosphere of Antigua, we have taken the value of refractive index $m = 1.33 - 0i$. This is not a severe limitation to our computations since Braslau and Dave (1973) have reported that in near ultraviolet the aerosol scattering optical thickness varies negligibly with a change in the real part of m.

Figures 10a and 10b depict the computed phase function $P(\theta)$ normalized to 4π (i. e. $\iint P d\omega = 4\pi$) for the maritime and continental size distributions respectively. Curves labeled B in 10a and 10b correspond to ordinates at the right and represent the cumulative phase defined as

$$\frac{F(\theta)}{F(\pi)} = \frac{1}{2} \int_0^\theta P \sin\theta \, d\theta \qquad (5)$$

They allow to read out the magnitude of scattering as a function of scattering angle θ. As for Figure 10b only about 43% of the total scattering takes place within 20° of the scattering angle. However the ratio of forward to backward scattering is quite high with about 93% of the photons scattered within 90° of the forward direction. For the maritime aerosols (Fig. 10a) the proportions are somewhat different with about 55% of the scattering taking place within first 20°. Figure 10a also shows that about 95% of the ultraviolet sunlight is scattered within 90° by the maritime aerosols.

Figures 11a and 11b represent the probability density of scattering volume cross sections. Curve A is probability density function p. d. f.
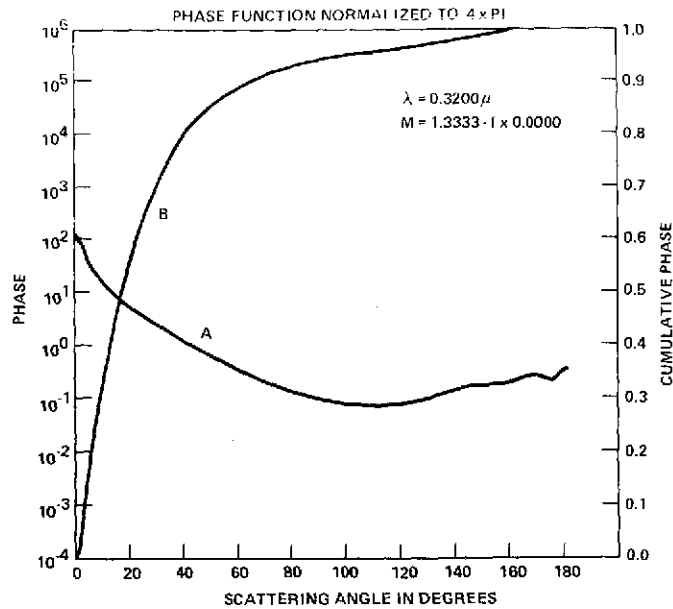
19

Figure 10a. Phase function (A) normalized to 4π is computed using maritime aerosol size distribution (Fig. 9). Curve B represents cumulative phase
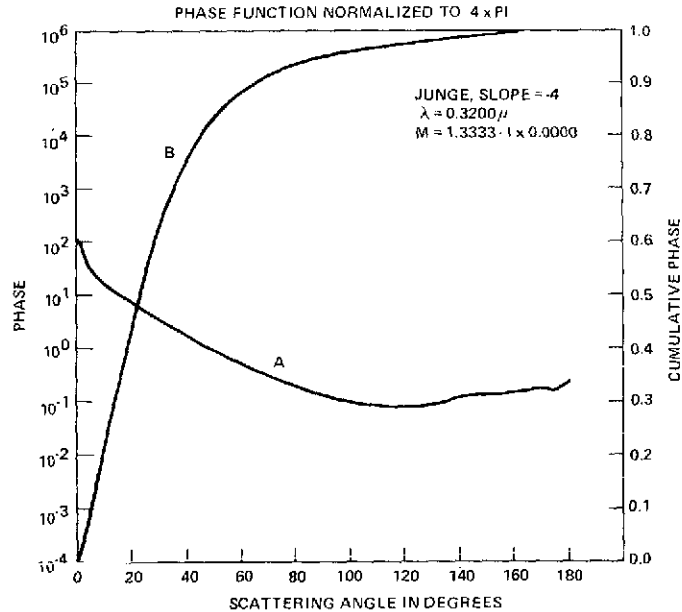

Figure 10b. Phase function (A) normalized to 4π is computed using aerosol distribution as given in Fig. 8. Curve B represents cumulative phase

20

PROBABILITY DENSITIES OF VOLUME CROSS SECTIONS

LOG NORMAL
$\lambda = 0.3200\mu$
M = 1.3333 - I x 0.0000

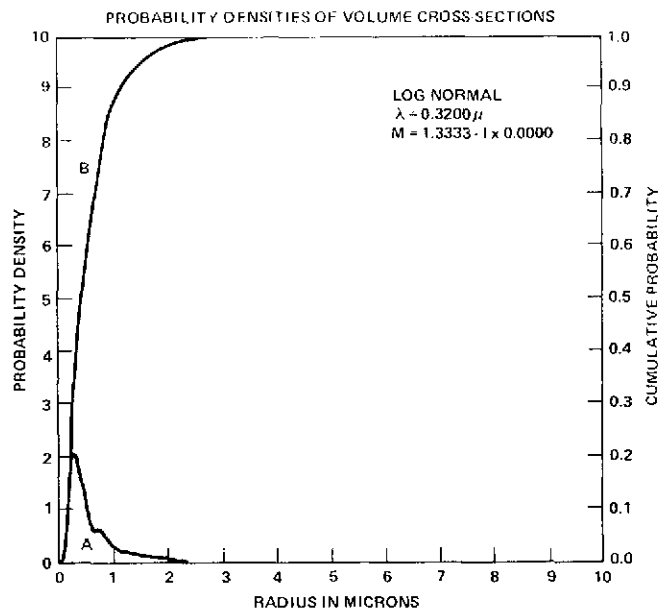PROBABILITY DENSITY

CUMULATIVE PROBABILITY

RADIUS IN MICRONS

Figure 11a. The probability density of extinction (Curve A) and the cumulative probability of extinction (B) as a function of radius of maritime aerosols. $\lambda = 3200$Å

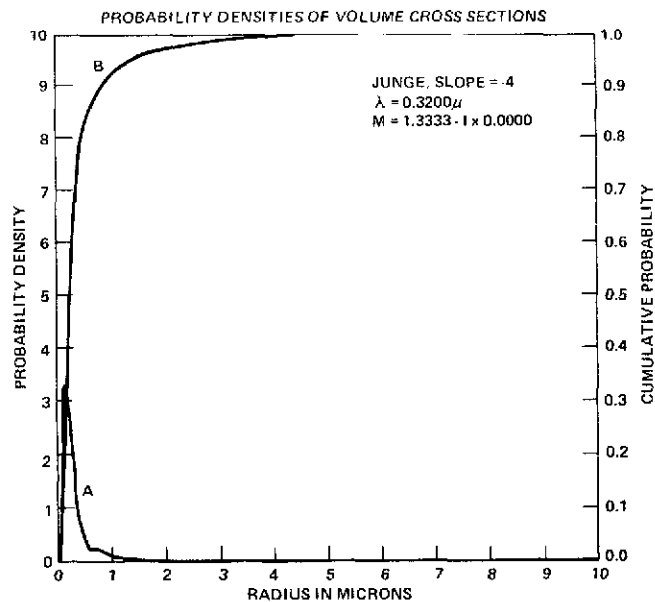PROBABILITY DENSITIES OF VOLUME CROSS SECTIONS

JUNGE, SLOPE = -4
$\lambda = 0.3200\mu$
M = 1.3333 - I x 0.0000

PROBABILITY DENSITY

CUMULATIVE PROBABILITY

RADIUS IN MICRONS

Figure 11b. The same as Fig. 11a but for continental aerosols (Fig. 8)

21

$$\text{P.d.f.} = \frac{\sigma_s(r) \, P(r, \theta) \, n(r)/4\pi}{\Sigma_s(\theta)} \tag{6}$$

where

$\sigma_s(r)$ = scattering cross section as a function of radius r of particles

$P(r, \theta)/4\pi$ = phase function

$$\Sigma_s(\theta) = \int_0^\infty \sigma_s(r) \, \frac{P(r, \theta)}{4\pi} \, n(r) \, dr$$

$n(r)$ = number of aerosols

P. d. f. shows that the aerosols with $0.16 \, \mu$m and $0.25 \, \mu$m radius would have the strongest interaction with the sunlight at $\lambda = 3200$Å. Curves B in Figures 11a, 11b represent the cumulative extinction probability Q (r) defined as

$$Q(r) = \frac{\Sigma(r)}{\Sigma(5\mu)} \tag{7}$$

where

$$\Sigma(r) = \int_0^r \sigma_{ext} \, n(r) \, dr$$

It can be seen that although the size range of aerosols is over several orders of magnitude, aerosols with radii between $0.1 - 1 \, \mu$m have a significant interaction with ultraviolet sunlight. This is true for both maritime and continental aerosol distribution, although the mass of larger particles $(r > 1\mu)$ is much higher in the maritime aerosol distribution than the given continental size spectrum. This fact is illustrated by Curve B in Figures 8 and 9, which represents the cumulative mass m(r) of aerosols

$$m(r) = \int_0^r \rho \, \frac{4}{3} \pi \, r^3 n(r) \, dr \quad ; \quad \rho = \text{density of aerosols}$$

It is interesting to investigate which of the aerosol sizes would be most effective in forward scattering ($\theta = 0°-10°$) of uv-sunlight. For this reason Figures 12a and 12b are computed. They represent the probability density of phase function defined as eq. 6.

It can be seen from 12a and 12b that aerosols that scatter ultraviolet radiation most effectively in the forward direction for an overhead sun ($Z \sim 0°$) would have a radius between $0.2 - 0.32\,\mu$m. This is a significant result for the measurement of ultraviolet radiation in maritime atmosphere, since Junge (1972) and Jaenicke et al. (1971) have reported from their aerosol measurement expeditions over the Atlantic that the main portion of the maritime aerosol consists of insoluble particles with a maximum range between $0.2 - 0.3\,\mu$m radius.

PROBABILITY DENSITY OF PHASE FUNCTION

LOG NORMAL
$\lambda = 0.3200\mu$
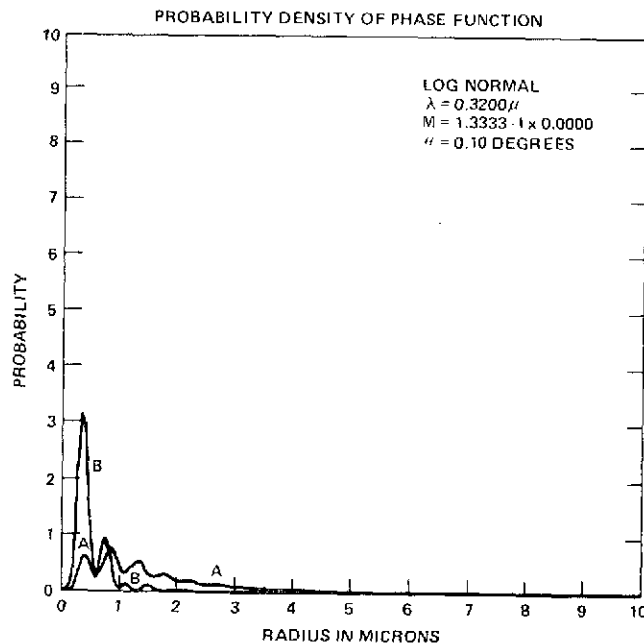M = 1.3333 · I × 0.0000
θ = 0.10 DEGREES

Figure 12a.   The probability densities of sunlight at 3200Å scattered in the directions 0° and 10° as function of radius of maritime aerosols (Fig. 9). Curve A corresponds to 0° and B to 10°

23

PROBABILITY DENSITY OF PHASE FUNCTION

JUNGE, SLOPE = -4
$\lambda = 0.3200\mu$
M = 1.3333 - I x 0.0000
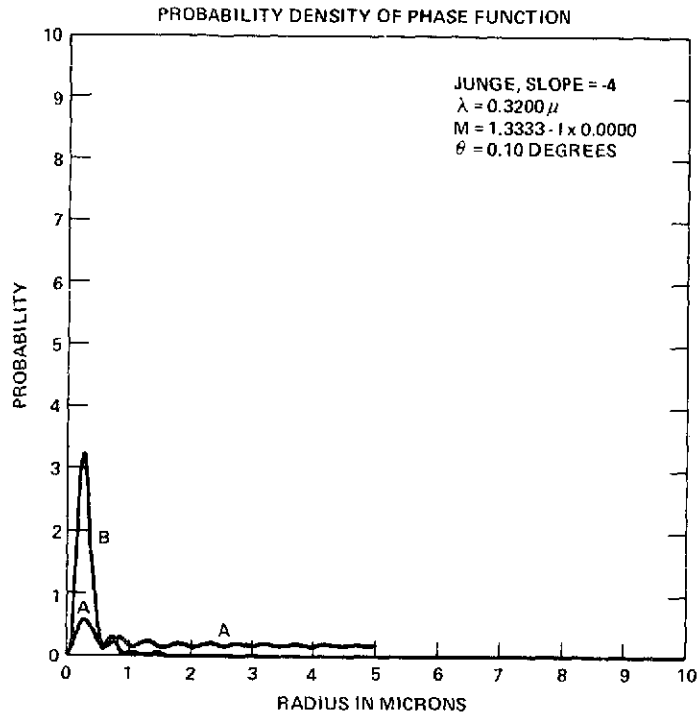θ = 0.10 DEGREES

PROBABILITY

RADIUS IN MICRONS

Figure 12b.   The probability densities of sunlight at 3200Å scattered in the directions 0° (Curve A) and 10° (Curve B) as a function of radius of continental aerosols (Fig. 8)

6.   CONCLUDING REMARKS

The present study indicates that forward scattering should have an appreciable effect on the ultraviolet sunlight especially in the maritime atmosphere. Determination of atmospheric ozone values by the measurement of solar uv-radiation is therefore subject to correct knowledge of magnitude of aerosol scattering at used wavelengths.

The discrepancy between measured and computed radiation profiles near to the surface is of the order of 20% and at the level of 15 km about 10%. Even after correcting for a probable maximum error of 6% in observations and 2% in

24

computations, one is still observing 12% more radiation near the surface and about 2% at 15 km. We believe this to be due to a strong contribution by forward scattering to the measured flux and to some extent due to undetectable stray light. Our results show that measured ultraviolet radiation profiles can be satisfactorily compared to the theoretical model calculations of radiative transfer.

The feasibility of employing the discussed measurement technique to the determination of directly transmitted ultraviolet sunlight is successfully demonstrated. It is desirable that such measurements be made at different wavelengths in the near ultraviolet at sites where the described technique is applicable ($20°$N-$20°$S). The rocket-payload can be made capable to measure radiation profiles at four wavelengths between 3200-4000Å by merely replacing the narrow-band spectral filters. In this way size and height distribution of aerosol can be derived (see e.g. de Barry and Rössler 1966) and more light can be shed on the behaviour of atmospheric aerosols interacting with uv-sunlight.

It is interesting to note that the atmosphere in the region of Antigua is affected by Sahara dust. Similar to radiation measurements made by Volz (1970) in this region, it is difficult to say how our measurements are affected by the Saharan dust. Future measurements at several ultraviolet wavelengths would also be useful to investigate this phenomena.

ACKNOWLEDGMENTS

REFERENCES

1. Bary, E. de and F. Rössler. 1966. Size distribution of atmospheric aerosols derived from scattered radiation measurements aloft. Jour. Geophy. Res. 71, 1011-1016

2. Braslau, N. and J. V. Dave. 1973. Effect of aerosols on the transfer of solar energy through realistic model atmospheres. Part I: Non-absorbing aerosols. J. Appl. Meteor. 12, 601-615

3. _____ 1973. Part III: Ground level fluxes in the biologically active bands 0.28-.37 u. Rept. RC 4308, IBM Res. Center, Yorktown Heights, N.Y.

4. Dave, J. V. 1972. Development of programs for computing characteristics of ultraviolet radiation. Techn. Reports IBM

5. Deirmendjian, D. and Z. Sekera. 1956. Atmospheric turbidity and transmission of ultraviolet sunlight. J. Opt. Soc. Amer. 46, 565-571

6. Eiden, R. and G. Eschelbach. 1973. Das atmosphärishe Aerosol und seine Bedeutung für den Energiehaushalt der Atmosphäre. Zeitschrift f. Geophysik, 39, 189-228

7. Furukawa, P. M. and D. F. Heath. 1973. The apparent spectral ultra-
    violet reflectances of various natural surfaces. Submitted for publication

8. Georgii, H. W. and G. Gravenhorst. 1972. Untersuchungen zur Konstitution
    des Aerosols über dem Atlantischen Ozean. Met. Rdsch. 180-181

9. Ghazi, A. 1973. Inference of total ozone from photometric measurements
    of sky radiation. PAGEOPH, 106-108, 950-961

10. Guschchin, G. P. 1968. Spectrophotometric investigations of the charac-
    teristics of atmospheric aerosols in various geographic regions of the
    USSR. Tr. Glar. Geof. Observ. No. 223

11. Jaenicke, R., C. Junge and H. J. Kanter. 1971. Messungen der Aerosol-
    grössenverteilung über dem Atlantik. "Meteor" Forsch. Erg. B7, 1-54

12. Krueger, A. J. and W. R. McBride. 1968. Rocket-ozonesonde (ROCOZ)
    Design and development. Naval Weapons Center, China Lake, NWC-TP
    4512

13. Krueger, A. J. 1969. Rocket measurements of ozone over Hawaii.
    Ann. Geophys. t 25, fasc. 1, 307-311

14. McClatchey, R. A., R. W. Fenn, J. E. A. Selby, F. E. Volz, J. S. Garing.
    1971. Optical properties of the atmosphere. AFCRL-71-0279

15. Paetzold, H. K. 1961. Messung des atmosphärischen Ozons. Hdb. Aero-
    logie. ed. W. Hesse, Akad. Verlag, Leipzig, 458-531

16. Pettit, E. 1932. Measurements of ultraviolet solar radiation. Astrophys. J. 75, 185

17. Rodionov, S. F., Ye. N. Pavlova, Ye. V. Rdultovskaya and N. M. Reynov. 1942. The selective transparancy of atmospheric aerosols. Izv. Akad. Nauk SSSR ser. Geogr. i. Geofiz. 6, 135

18. Rodionov, S. F. 1950. Transparancy of the atmosphere in the ultraviolet. Ibid., 14, No. 4, 1950

19. Roosen, R. G., R. J. Angione and C. H. Kleincke. 1973. Worldwide variations in atmospheric transmission: 1. Baseline results from Smithsonian observations. Bull. Amer. Met. Soc., vol. 54, 4, 307-316

20. Volz, F. E. 1970. Spectral skylight and solar radiance measurements in the Caribbean: Maritime aerosols and Sahara dust. J. Atm. Sci. 27, 1041-1047